

Morphology and physical properties of poly(styrene-*b*-isobutylene-*b*-styrene) block copolymers

Robson F. Storey* and Bret J. Chisholm†

Department of Polymer Science, The University of Southern Mississippi, Hattiesburg, MS 39406-0076, USA

and Michael A. Masse

Shell Development Company, Westhollow Technology Center, Houston, TX 77251-1380, USA
(Received 6 September 1994; revised 30 October 1995)

A series of linear and three-arm star poly(styrene-*b*-isobutylene-*b*-styrene) (PS-PIB-PS) block copolymers with varying block compositions was synthesized via living carbocationic polymerization using the initiation system 1,3-di(2-chloro-2-propyl)-5-*tert*-butylbenzene (or 1,3,5-*tris*-(2-chloro-2-propyl)benzene)/TiCl₄/pyridine/2,6-di-*tert*-butylpyridine in a 60/40 (v/v) hexane/MeCl solvent mixture at -80°C. High resolution gel permeation chromatography showed that the compositions of the copolymers were complex, consisting of higher molecular weight coupled products, and products of lower molecular weight including, probably, homo-PS. Morphology and physical properties were characteristic of microphase-separated block copolymers, and were affected strongly by the PIB span molecular weight and volume fraction of PS. When the latter was in the range 0.20–0.42 vol%, the morphology was characterized by cylinders of PS in a continuous phase of PIB; however, at least two samples exhibited mixed morphologies in which regions of PS cylinders coexisted with regions of PS spheres and lamellae, respectively. Linear samples showed much better long-range morphological order than star-branched samples. The dynamic mechanical response of block copolymers consisted of separate PIB and PS relaxations whose relative intensities scaled well with copolymer composition. The low-temperature relaxation was broad, which is an inherent characteristic of PIB; the high-temperature PS relaxation was narrow, suggesting well defined phase separation and a sharp PIB-PS interface. Melt rheological studies of representative samples showed that microphase separation persisted up to 265°C. Tensile properties varied with PIB span molecular weight and PS content. An abrupt change occurred from 15–22 vol% PS, indicating a minimum PS content needed for strong network formation. Properties changed from elastomeric within the range 20–37 vol% PS, to ductile in the range 37–45 vol%, to brittle in the range 45–55 vol%. Samples with PS vol% ≥ 35 yielded improved elastomeric properties as a result of annealing above the glass transition temperature of PS. Within the elastomeric range, the PIB span molecular weight was the dominant factor effecting elongation at break. A high tensile strength of 24 MPa was obtained, and most samples displayed strengths ≥ 15 MPa. Copyright © 1996 Elsevier Science Ltd.

(Keywords: polyisobutylene; poly(styrene-*b*-isobutylene-*b*-styrene); block copolymer)

INTRODUCTION

There exists a great deal of interest in A-B-A block copolymers¹, both academic and industrial, that can be attributed to the unique morphology these materials exhibit in the bulk state. The immiscibility of the outer blocks with the inner block results in phase separation and the formation of a heterophase morphology. Since these blocks are connected to each other by covalent bonds, the phase separation that occurs is characterized by the formation of small microdomains of the minor (low volume fraction) block in a continuous phase of the major (high volume fraction) block. Furthermore, depending on the volume ratio of the two blocks, the phase morphology can vary dramatically².

An especially important type of A-B-A block copolymer possesses, at ambient temperature, A blocks that are glassy and a B block that is rubbery. Such block copolymers fall within the general class of polymeric materials termed thermoplastic elastomers (TPEs), since, when placed under stress, they behave much like a high-strength vulcanized rubber, but at high temperatures can be processed much like a conventional thermoplastic polymer. One of the more important commercial TPEs is poly(styrene-*b*-diene-*b*-styrene) A-B-A block copolymers in which the polydiene mid-block is polybutadiene or polyisoprene of appropriate microstructure. These materials are produced via living anionic polymerization using a sequential addition of monomers. The presence of one double bond per repeat unit in the diene mid-block of these TPEs severely limits their thermal and oxidative stability; consequently, they must be subjected to a post-polymerization hydrogenation to obtain the

* To whom correspondence should be addressed

† Present address: The General Electric Company, Mount Vernon, IN, USA

thermal and oxidative stability required for some applications.

Recently, the advent of living or long-lived carbocationic polymerization of alkenes³⁻¹³ has enabled the synthesis of block copolymer compositions, particularly well-defined polyisobutylene (PIB)-based block copolymers¹⁴⁻²⁰, not accessible through conventional living anionic polymerization. Thus, new property sets of block copolymers are achievable. Kennedy and coworkers have synthesized a number of A-B-A block copolymers possessing a PIB mid-block and various glassy outer-blocks, including polystyrene (PS)¹⁴, poly(*p*-chlorostyrene)¹⁵, poly(*p*-methylstyrene)^{16,17}, poly(*p*-*tert*-butylstyrene)^{16,18}, and polyindene^{16,19}. This new class of TPE possesses an inherently totally saturated inner block, which has been shown to yield much higher thermal stability than commercially available hydrogenated poly(styrene-*b*-butadiene-*b*-styrene)²⁰. It is also well known that PIB-based elastomers provide superior oxidative and chemical stability, and for certain applications, PIB-based triblocks would be expected to yield barrier and damping properties that cannot be obtained with diene-based materials.

The new living carbocationic polymerization is brought about either by careful selection and use of a counterion of suitable nucleophilicity^{3,21}, or by external addition to^{6-8,10-23} or *in situ* formation within^{4,5,18,21,22,24,25} the polymerization mixture of a Lewis base, i.e. an electron donor, which, due to steric reasons, may or may not^{12,13} be capable of complexation with Lewis acid coinitiators. The synthesis of linear and three-arm star PIB-based block copolymers, using sequential addition of monomers, has been accomplished predominantly through the external electron donor method, in the presence of a conventional cationogen/Lewis acid initiation system, using various complexing Lewis bases such as dimethylsulfoxide, dimethyl acetamide, or pyridine, or the non-complexing di-*tert*-butylpyridine (DTBP). The precise function of the externally added electron donor is currently under debate. Since the presence of the Lewis base causes a dramatic decrease in the overall rate of polymerization, 'cation stabilization'²² has been suggested leading to the creation of an equilibrium between a large number of dormant covalent (reversibly terminated) or onium chain ends, and a small number of active ion pairs^{8,9,22}. Conversely, others have suggested that the main function of complexing electron donors, and the sole function of non-complexing electron donors such as DTBP is to trap protons or protic impurities, e.g., water, in the polymerization system^{12,13,23}.

When the effectiveness of Lewis-base-mediated living carbocationic polymerization is compared to that of living anionic polymerization for the synthesis of TPEs, it can be seen that, in general, the cationic process does not provide as well-defined polymers as does the anionic process as evidenced by the broader molecular weight distributions and less regular phase-separated morphologies exhibited by PIB-based TPEs^{14,15}. The principle reasons for this are, competing initiation of polymer chains by protic impurities, Friedel-Crafts alkylation of styryl aromatic rings by growing carbocations, and the existence of a unimolecular β -proton elimination reaction (gegen-ion assisted chain transfer) of slow but finite rate. The

existence of the latter reaction is suggested by the observation that for the living polymerization of IB, a deviation from living characteristics becomes apparent at high monomer conversion^{8,12,19,20,24,25}. However, it has been shown recently, for the synthesis of poly(styrene-*b*-isobutylene-*b*-styrene) (PS-PIB-PS) block copolymers using the 1,4-*bis*-(2-chloro-2-propyl)benzene (dicumyl chloride) (DCC)/TiCl₄/pyridine initiation system, that by carefully controlling the time of addition of styrene to living PIB di- or tri-cations and by adding the proton trap, 2,6-di-*tert*-butylpyridine (DtBuP), to the reaction mixture, PS-PIB-PS block copolymers can be produced that approach the narrow molecular weight distributions and well-defined morphologies exhibited by poly(styrene-*b*-diene-*b*-styrene) block copolymers produced by living anionic polymerization²⁷. In this paper are described the morphology and physical properties of PS-PIB-PS block copolymers that have been prepared according to this method.

EXPERIMENTAL

Materials

Hexane (Aldrich Chemical Co.) was distilled from calcium hydride just prior to use. Isobutylene (IB) and methyl chloride (Linde Div., Union Carbide Corp.) were dried by passing the gaseous material through a column packed with BaO and CaCl₂. Styrene (Aldrich) was distilled from calcium hydride under vacuum and stored under nitrogen for no longer than one day before use. Titanium tetrachloride, pyridine, 2,6-di-*tert*-butylpyridine, and anhydrous methanol (all Aldrich) were used as received.

1,3-Di(2-chloro-2-propyl)-5-*tert*-butylbenzene (*t*Bu-DCC) was synthesized from 5-*tert*-butylisophthalic acid (Amoco Chemical Co.) using the following reaction sequence: 1) esterification with two moles of ethanol²⁴, 2) reaction of the resulting diester with four moles of methylmagnesium bromide²⁴, and 3) chlorination of the resulting 1,3-di(2-hydroxy-2-propyl)-5-*tert*-butylbenzene with gaseous HCl⁸. The latter reaction was also used to produce DCC from 1,4-*bis*-(2-hydroxy-2-propyl)benzene (Goodyear Tire and Rubber Co.). The preparation of 1,3,5-*tris*-(2-chloro-2-propyl)benzene (tricumylchloride) (TCC) has also been described⁸.

Polymerization

Linear and three-arm star PS-PIB-PS block copolymers of various compositions were synthesized using the DCC, *t*Bu-DCC, or TCC/TiCl₄/pyridine initiating system in a 60/40 (v/v) hexane/methyl chloride solvent system at -80°C, with a small concentration of DtBuP present as a proton trap. Specific polymerization conditions for the synthesis of the various block copolymers are listed in *Table 1*. The samples are each designated by three hyphenated numbers, *n-x-y*, where *n* is the number of arms, either two for a linear or three for a three-arm star block copolymer, and *x* and *y* are the molecular weights in thousands of daltons, of the PIB and PS segments, respectively, of each arm. In every case, the living PIB block was formed first by the addition of neat TiCl₄ to a hexane/methyl chloride solution of IB, initiator, pyridine, and DtBuP. The molar ratios of pyridine to initiator, and TiCl₄ to initiator, were approximately 2:1 and 20:1, respectively, for DCC

Table 1 Polymerization conditions for the synthesis of PS-PIB-PS block copolymers

Sample	[DCC] (M × 10 ³)	[tBu-DCC] (M × 10 ³)	[TCC] (M × 10 ³)	[DTBP] (M × 10 ³)	Initial rxn. vol. (l)	Later IB additions		Styrene addition ^a			Termination	
						mol	min	IB conv. ^b	mol	min	Sty. conv. ^c	min
2-14-3	–	1.88	–	1.0	1.60	–	–	0.94	0.873	103	0.19	131
2-29-9	2.04	–	–	–	0.584	4 × 0.317	20, 40, 60, 80	0.67	0.349	220	0.60	156
2-25-12	–	1.88	–	1.0	1.60	0.80	20	0.83	0.873	145	0.77	205
						0.80	40					
2-16-10	–	1.88	–	1.2	0.25	0.127	20	0.53	0.174	150	0.51	210
						0.127	40					
2-15-12	–	1.88	–	1.2	0.25	0.127	20	0.67	0.174	120	0.63	180
2-16-13	–	1.88	–	1.0	1.60	0.80	20	0.72	0.873	121	0.88	151
2-14-13	–	1.88	–	1.2	0.25	0.127	20	0.62	0.349	120	0.34	180
2-20-28	–	1.88	–	1.0	0.25	0.127	20	0.66	0.349	150	0.73	210
						0.127	40					
3-23-7	–	–	1.25	1.0	1.60	0.80	20	1.04	0.873	121	0.45	157
3-12-8	–	–	1.25	1.0	1.60	–	–	0.81	0.873	104	0.54	132

^a Added as a 4.4 M solution in 60/40 (v/v) hexane/methyl chloride

^b Calculated from g.p.c.-estimated M_n of PIB block prior to styrene addition

^c Calculated from n.m.r.-estimated M_n of PS blocks

For all reactions: [IB]₀ = 1.00 M; $T = -80^\circ\text{C}$; [Pyr] = 2[DCC] or 2[tBu-DCC] or 3[TCC]; solvent = 60/40 (v/v) hexane/methyl chloride; [TiCl₄] = 10[Pyr]

and tBu-DCC, and 3 : 1 and 30 : 1, respectively, for TCC. For polymerizations in which higher polyisobutylene molecular weights were desired, additional charges of isobutylene were made to the reaction mixture at regular intervals during the polymerization.

The appropriate time for styrene addition was determined by removing aliquots from the isobutylene reaction mixture, quenching them with methanol and observing their peak elution times in g.p.c. (gel permeation chromatography) traces. When the peak elution times of polymers formed at successive time intervals was found to be essentially the same or very close to the same, a hexane/methyl chloride solution of styrene was added to the reaction mixture and allowed to polymerize. After a certain time, determined from experience, the polymerization was stopped by the addition of methanol to the reaction mixture.

Polymerizations were carried out under dry nitrogen, in a glove box equipped with an integral cold-temperature bath. A representative procedure for the synthesis of a linear PS-PIB-PS block copolymer was as follows: Into a chilled 2000 ml three-neck, round-bottomed flask equipped with a mechanical stirrer were charged 629 ml MeCl and 944 ml hexane. From this solution, 100 ml was removed and placed into a chilled 250 ml round-bottomed flask via a 50 ml volumetric pipette. To the remaining solution, 126 ml (1.60 mol) isobutylene, 0.48 g (6.1×10^{-3} mol) pyridine, 0.30 g (1.6×10^{-3} mol) DtBuP, and 0.863 g (3.01×10^{-3} mol) tBu-DCC were added and stirred for approximately 20 min. To the 250 ml round-bottomed flask which contained 100 ml of mixed solvent, was added 100 ml (0.871 mol) styrene.

Polymerization was initiated by the rapid addition of 6.7 ml neat TiCl₄ to the reaction mixture with vigorous stirring. After a reaction time of 20 min, an additional 63 ml (0.80 mol) of IB was added to the reaction mixture, and aliquots were subsequently removed and quenched

with methanol, at approximately 15-min intervals. Molecular weight build-up of polymers removed was determined by g.p.c. by observing the elution time corresponding to the peak in the distribution. At a reaction time of 121 min, the 200 ml pre-chilled styrene solution was added to the reaction mixture, and polymerization was continued for an additional 30 min at which time the polymerization was quenched with approximately 60 ml of pre-chilled methanol.

The reaction vessel was removed from the glove box, placed in a hood, and allowed to warm to room temperature, with stirring to ensure smooth evaporation of methyl chloride. Additional hexane (600 ml) was added and the solution was slowly precipitated into a large excess of methanol. The precipitate was collected by decanting the solvent, redissolved in tetrahydrofuran (THF), reprecipitated into methanol, and dried *in vacuo* at 80°C for 3 days.

Film preparation

For static tensile measurements and dynamic mechanical analysis (d.m.a.), film samples were cast from THF solutions (10–20 wt%) of the block copolymers. The solutions were poured into Teflon-coated aluminium pans, the pans were covered with aluminium foil containing several small pin holes, and the solvent was allowed to evaporate at room temperature under atmospheric pressure. Once dry to the touch, the films were removed from the pans and placed in a vacuum oven for a few days using initial temperatures in the range 40–60°C, under a slight vacuum to prevent bubbling of the films, and subsequently at 60°C using a high vacuum. Samples containing high PS contents (≥ 35 vol%) were additionally annealed at 110°C for 24 h under high vacuum, with exception of sample 3-12-8, that was annealed for tensile measurements, but not for d.m.a. The range of thickness of the films was 0.25–1.0 mm.

For melt rheology, differential scanning calorimetry (d.s.c.), and microscopy studies, samples were cast from toluene (10 wt%) into teflon-coated aluminium pans over a 7–10 day period. The films were further dried *in vacuo* for 24–48 h and then annealed at 130°C for 2 h. The thickness of the resulting films ranged from 0.5 mm to 1.5 mm.

Instrumentation

¹H n.m.r. spectra were obtained using a 200 MHz Bruker ACE-200 n.m.r. spectrometer. Samples were prepared in CD₂Cl₂. Peak positions were reported against the internal reference of CH₂Cl₂ at 5.32 ppm.

G.p.c. was used to determine molecular weights and molecular weight distributions (*MWDs*) of polymer samples, using narrow-polydispersity PIB standards as a reference. Routine g.p.c. analysis was carried out using a Waters Associates GPC system equipped with a Rheodyne injector, a Waters model 510 HPLC solvent delivery pump, three Ultrastaygel columns of nominal pore sizes 500, 10³, and 10⁴ Å, and a Waters model 410 differential refractometer detector operating at 33°C. THF, freshly distilled from calcium hydride, served as the mobile phase, and was delivered at a flow rate of 1.0 ml min⁻¹. Sample concentrations were approximately 0.5% (w/w) in THF, with an injection volume of 50 ml. In some cases, high resolution g.p.c. was carried out using a Shell Development Co. proprietary system, which employed a THF mobile phase at 50°C and dual refractive index and ultraviolet detectors. These g.p.c. results were curve-resolved using Peakfit software by Jandel Scientific.

Scanning transmission electron microscopy (STEM) was carried out using a Jeol 100CX instrument equipped with a Temscan attachment applied to cryo-ultramicrotomed samples of 800–1000 Å thickness. Polystyrene domains were stained after sectioning with RuO₄. The microscope was operated at 100 kV.

Differential scanning calorimetry (d.s.c.) was carried out using a DuPont 2100 DSC; sample size was 15–20 mg. The sample was cooled to –100°C and then heated at 20°C min⁻¹ up to a temperature of –20°C. Measurements were done on the second heating cycle of the sample to ensure that all samples had the same thermal history. The glass transition temperature (*T_g*)

was determined as the midpoint of the step change in the heat capacity.

D.m.a. spectra were obtained using a Seiko model SSC/5200H dynamic mechanical spectrometer equipped with a DMS 210 tension module. Rectangular samples possessing gauge lengths of 20 mm and widths in the range of 5–8 mm were used for testing. Spectra were obtained by performing a temperature sweep at a constant frequency of 1 Hz.

Melt rheology was measured using a Rheometrics Mechanical Spectrometer Model 605. Samples of approximately 1 mm thickness were placed between 12.5 mm radius parallel plates. The frequency response was recorded at several temperatures. A strain amplitude of 3.0% was chosen so that testing occurred in the linear viscoelastic region.

Tensile properties were measured using an MTS Model 810 Universal Test Machine. Micro-dumb-bell samples possessing a gauge length of 11.00 mm and a width of 1.54 mm were stamped from films ranging in thickness from 0.25 to 1.0 mm. A 100 lb load cell with a 100 lb load range cartridge and a 10 in displacement cartridge were used in conjunction with a 1 mm s⁻¹ continuous strain rate to obtain tensile data.

RESULTS AND DISCUSSION

Linear and three-arm star radial PS-PIB-PS block copolymers of various block molecular weights were synthesized to study the effects of composition on block copolymer physical properties. Ten samples were synthesized, and their compositions are described in Table 2.

Synthesis of PS-PIB-PS block copolymers

The initiating systems used to produce linear and three-arm star block copolymers were (*t*Bu-DCC or DCC)/TiCl₄/pyridine and TCC/TiCl₄/pyridine, respectively. The solvent system used was a 60/40 (v/v) hexane/methyl chloride mixture, and the polymerization temperature was –80°C. *DtBuP* was added to the polymerization medium, since it has been shown that this compound results in narrower molecular weight distributions by trapping protons that are present as impurities and which result from side reactions during polymerization^{20,28}.

Table 2 Compositions of PS-PIB-PS block copolymers

Sample ID	\bar{M}_n PIB block (g mol ⁻¹)	<i>MWD</i> PIB block	Vol % styrene	Wt % styrene	\bar{M}_n PS block (g mol ⁻¹)	Overall <i>MWD</i>
2-14-3	28 000	1.25	15	17.1	2 900	–
2-29-9	58 000	1.16	22	24.1	9 200	1.32
2-25-12	49 700	1.17	29	31.9	11 650	1.40
2-16-10	31 800	1.33	35	38.0	9 750	1.39
2-15-12	30 000	1.20	41	44.5	12 050	1.85
2-16-13	32 100	1.15	42	45.4	13 350	1.47
2-14-13	27 800	1.26	45	48.3	13 000	1.67
2-20-28	39 700	1.46	55	58.5	28 000	1.43
3-23-7	70 200	1.22	20	22.7	6 870	1.22
3-12-8	36 500	1.23	37	40.1	8 130	1.36

Volume fraction of styrene was calculated from the measured (¹H n.m.r.) weight fraction and the following densities: $\rho_{PS} = 1.05 \text{ g cm}^{-3}$; $\rho_{PIB} = 0.92 \text{ g cm}^{-3}$

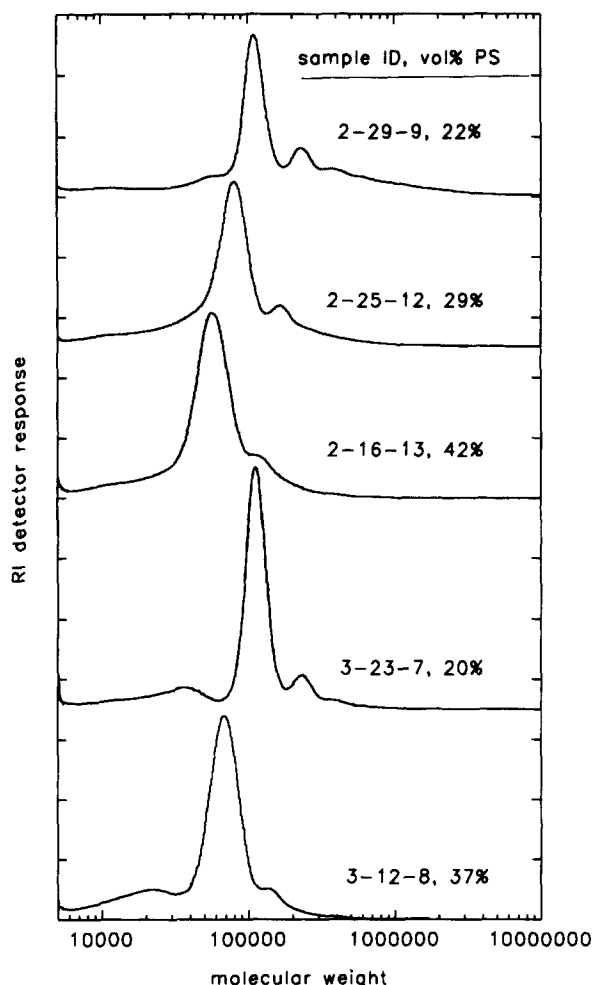


Figure 1 High resolution g.p.c. traces (RI detector) of selected PS-PIB-PS block copolymers

Isobutylene was polymerized to a relatively high conversion, and then styrene was added to produce the A-B-A block architecture. In cases where higher molecular weight PIB blocks were desired, one or two post-initiation IB charges were made at regular intervals to the reaction mixture. Incremental monomer addition allowed the monomer/initiator ratio to be initially lower than it would otherwise be for a given final molecular weight. Thus, the initiating system concentration can be higher than otherwise, allowing for faster rates of polymerization, and at the same time, monomer concentration can be lower than otherwise, thereby limiting the fraction of total hydrocarbon in the polymerization medium and allowing for faster initiation.

The time of addition of styrene to living PIB carbocations was determined by removing aliquots from the IB polymerization mixture as a function of reaction time, quenching them with methanol, and observing the peak elution times in their g.p.c. traces. When the peak elution times of successive PIB samples began to change only slightly with time, a hexane/methyl chloride solution of styrene was added to the polymerization mixture to affect the formation of polystyrene end blocks.

The molecular weight of polystyrene blocks was controlled by the amount of styrene added as well as the reaction time. The molecular weight and *MWD* of PIB blocks, as shown in *Table 2*, were determined by g.p.c. using samples removed from the polymerization mixture just prior to styrene addition. Styrene block molecular weight was determined using ^1H n.m.r. by integrating the area under the aromatic resonances relative to that of the aliphatic resonances. The overall *MWD* was determined by g.p.c. using a PIB calibration curve constructed from narrow *MWD* PIB standards. Considering the *MWD* values in *Table 2*, it can be seen

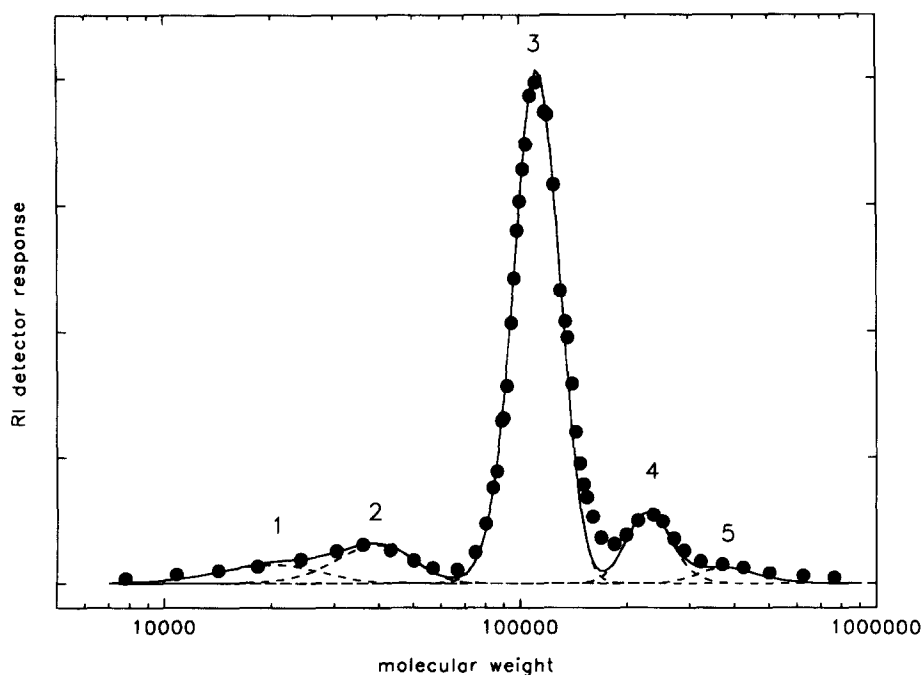


Figure 2 Curve-resolved high resolution g.p.c. trace (RI detector) of block copolymer 3-23-7 (● experimental data, --- curve components, — composite fit curve)

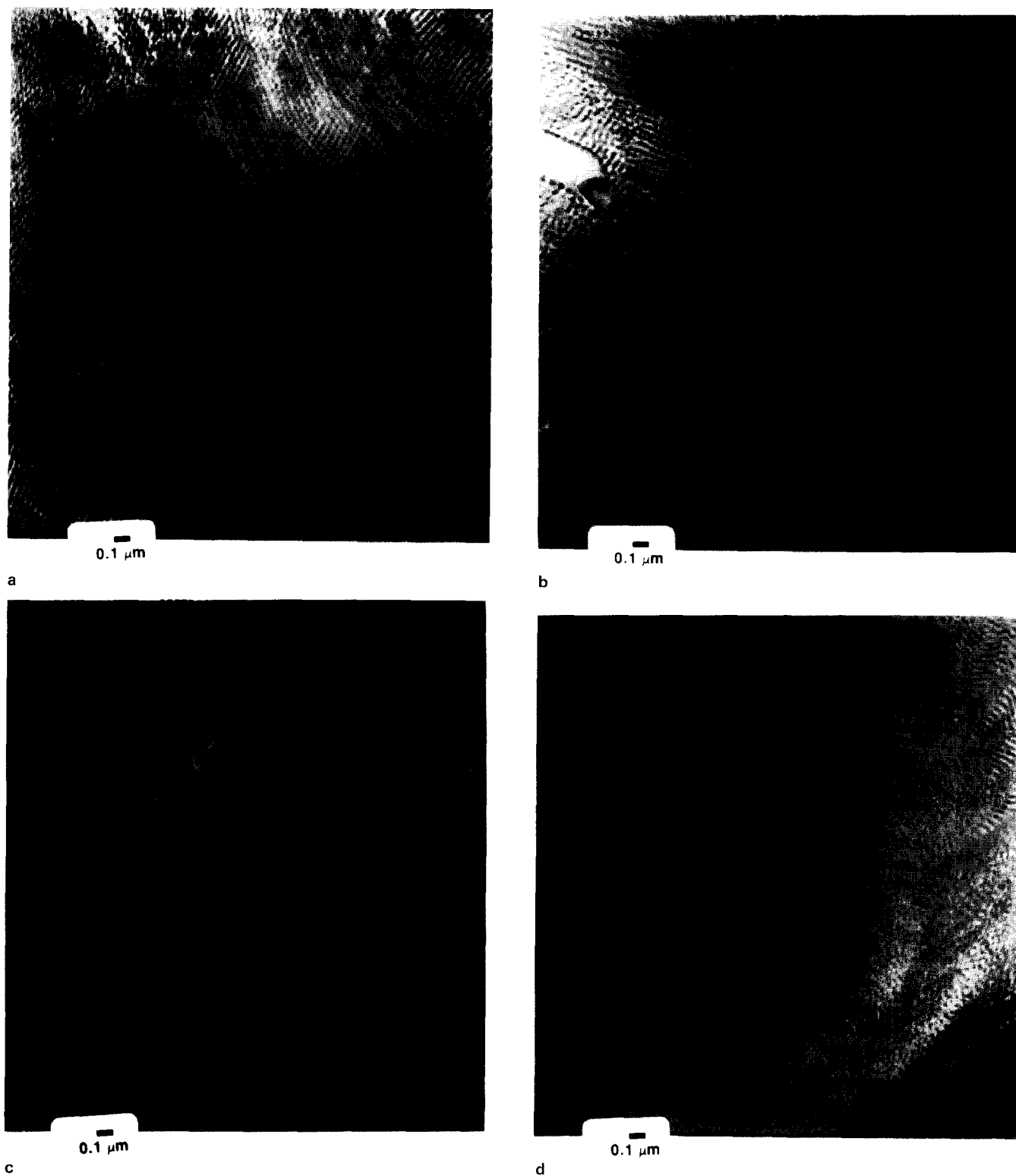


Figure 3 Transmission electron micrographs of PS-PIB-PS block copolymers: (a) 3-23-7; (b) 2-29-9; (c) 2-25-12 (first view); (d) 2-25-12 (second view); (e) 3-12-8; (f) 2-16-13

that, in general *MWDs* of the PIB mid-blocks were narrow but that broadening occurred during polystyrene block formation indicating the presence of side reactions in this step of the synthesis.

When comparing the g.p.c. traces of PIB mid-blocks to final block copolymers, it was often found that traces for the final block copolymer possessed a low elution volume (high molecular weight) shoulder that was not present in traces for PIB mid-blocks. High resolution g.p.c. was utilized to more fully characterize the various

molecular species present in the block copolymers. *Figure 1* shows the refractive index (RI) detector response for five selected samples. In general, this work showed that the compositions of the PS-PIB-PS block copolymers were more complex than was suggested by typical low-resolution g.p.c., and more work in this area will be necessary before detailed results can be published. However, some samples possessed simpler compositions and were more readily analysed by this technique. For example, *Figure 2* shows a curve-resolved high resolution



e



f

Figure 3 (Continued)

g.p.c. trace (RI detector) of sample 3-23-7. The major peak (3) represents the target block copolymer molecule. In addition, four minor peaks may be observed, two of which are higher and two of which are lower in average molecular weight than the major peak. The ultraviolet (u.v.) detector trace (not shown) is virtually identical to Figure 2, except for small differences in the relative intensities of the various peaks, the significance of which will be discussed below. The two highest molecular weight peaks (4 and 5), were found to possess molecular weights approximately twice (4) and three times (5) that of the main peak, strongly suggesting that they represent branched molecules formed through intramolecular ring-alkylation since the molecular weight would be expected to double as a result of one such ring-alkylation on a polymer, and to triple in the case of two. Additionally, the fact that the higher, branched fractions possess molecular weights which are almost perfect multiples of the main peak indicates that most of the branching occurred late in the styrene polymerization.

The origin of the other two minor peaks is less certain, although it is clear that none are PIB homopolymer since they all are also present in the u.v.-detector trace. This is sensible since it is highly unlikely that all three arms of a given molecule would fail in the cross-over to styrene propagation. Peak 1 is relatively stronger in the u.v. trace than the RI trace, suggesting that it is probably PS homopolymer. This is consistent with experience, since selective solvent extraction typically reveals a small but finite fraction of homo-PS in these PS-PIB-PS block copolymers^{20,27}. Peak 2 could be single 'arm' material since its molecular weight relative to polystyrene standards is just slightly higher than one-third of the three-arm star target molecule. It is tempting to hypothesize that this arm contaminant was produced by trifunctional initiator that initiated from only one site;

however, most mechanisms which might be suggested to explain this occurrence would also predict, statistically, that there would also be two-arm material produced by initiators that initiated from only two sites. Figure 2 clearly shows that such two-arm material is not present, however. Thus the exact origin of peak 2 remains unresolved. Using similar reasoning, polymers produced from difunctional initiator should show an arm contaminant that is approximately one-half of the target molecule. Of the three linear copolymers in Figure 1, only 2-29-9 shows such a contaminant, and notably, its peak position is exactly one-half the molecular weight of the target molecule. This particular polymer was produced from DCC, which has no blocking group on the aromatic ring, and so this contaminant probably results from intramolecular alkylation after addition of one isobutylene unit. Therefore, one must conclude that each type of initiator will produce a characteristic set of low molecular weight impurities, and their unequivocal identification will be addressed in future work.

PS-PIB-PS morphology

Samples 2-29-9, 2-25-12, 2-16-13, 3-23-7, and 3-12-8 were analysed using STEM, and all showed a microphase-separated morphology at room temperature. The micrographs shown in Figure 3 were used to characterize the block copolymer morphology with regard to type and degree of long-range order, and the results are summarized in Table 3. Because the image contrast was enhanced by RuO₄ staining, the dark and light microdomains are identified as the PS and PIB microdomains, respectively. Samples 3-23-7 (Figure 3a) and 2-29-9 (Figure 3b), having styrene volume fractions of 0.20 and 0.22, respectively, display hexagonally packed cylindrical morphologies. Samples 3-23-7, however, is relatively disordered while sample 2-29-9 shows excellent long range order. The morphological type found in

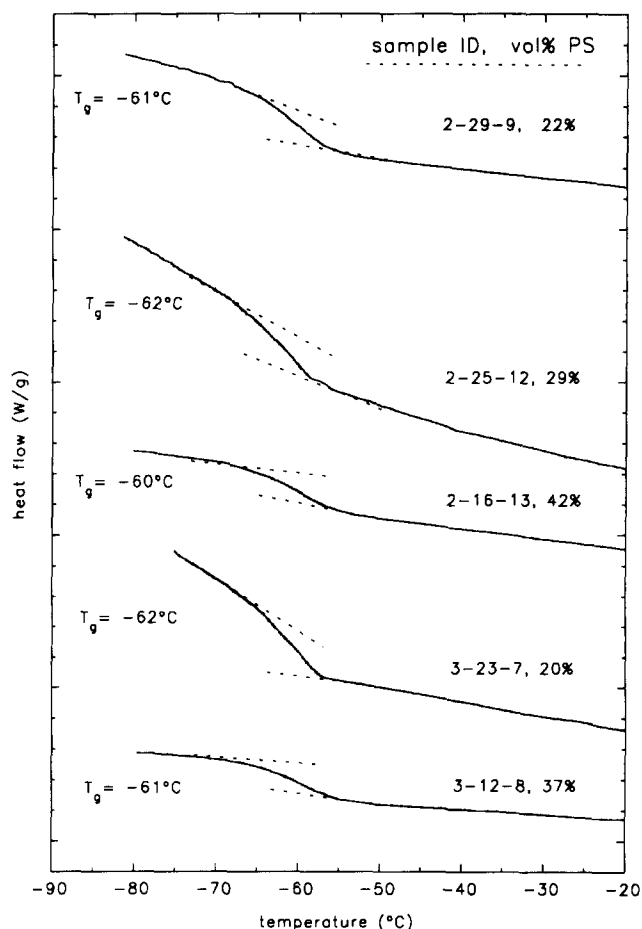
Table 3 Summary of morphology results

Sample ID	Vol% PS	Number of arms	Morphological type	Degree of long range ordering
2-29-9	22	2	cylindrical	excellent
2-25-12	29	2	spherical/cylindrical	excellent
2-16-13	42	2	cylindrical	good
3-23-7	20	3	cylindrical	poor
3-12-8	37	3	cylindrical/lamellar	poor

microphase-separated block copolymers is dependent upon the volume occupied by the two phases. At volume fractions between 0.18 and 0.28, hexagonally packed cylindrical morphologies are expected²⁹. Thus, samples 3-23-7 and 2-29-9 fit this expectation with the linear polymer showing a higher degree of order than the three-arm star. Some indication of unstained regions also exists in the micrograph of sample 2-29-9, and this is expected to be homo-PIB since the RuO₄ preferentially stains the PS domains. In fact, this particular sample showed a broad underlying peak in the high resolution g.p.c. spectrum (RI detector) that could possibly be attributed to homo-PIB.

The linear sample, 2-25-12, displayed a mixed morphology. *Figures 3c* and *3d* show different images collected from this sample. In *Figure 3c* the morphology is primarily hexagonally packed cylinders with both axial and radial projections visible. In *Figure 3d* the projected PS domains appear circular, and, while there are some regions having hexagonal symmetry, the majority of the image shows a square lattice projection. A radial projection of cylinders is not apparent in this image. These two projections in *Figure 3d* are consistent with a body-centred cubic arrangement of spherical polystyrene microdomains³⁰. In this interpretation the square lattice corresponds to the (100) projection and hexagonal lattice to the (111) projection. At a PS volume fraction of 0.29 a cylindrical morphology is expected. That the morphology is mixed between cylinders and spheres suggests that a distribution of compositions exists within the sample. For example, some of the local regions imaged in *Figure 3d* could possess PS volume fractions that are lower than the average due to the presence of poly(isobutylene-*b*-styrene) diblock copolymers or even possibly PIB homopolymer. These impurities could arise from termination of the growing chains before or shortly after cross-over to styrene monomer on either or both arms of the polymer.

Samples 3-12-8 and 2-16-13 have PS fractions of 0.37 and 0.42, respectively; at this composition lamellar morphologies are expected. Sample 3-12-8 (*Figure 3e*) has a lamellar or cylindrical morphology of poor long range order, and like sample 3-23-7, which also showed poor long range order, this sample has a three-arm star architecture. Sample 2-16-13 (*Figure 3f*) shows a cylindrical morphology with excellent long range order. In addition, the latter sample does have relatively large unstained regions which are likely homo-PIB. The presence of homo-PIB and the mixed and unexpected morphologies suggest some compositional irregularities in these samples, and this is consistent with the complex results obtained with high resolution g.p.c.

**Figure 4** D.s.c. results within the region of the PIB glass transition

Differential scanning calorimetry

The T_g of the PIB block of selected samples was studied using d.s.c. as shown in *Figure 4*. A clear step change in sample heat capacity was observed to occur in the range of -65°C to -55°C for samples representing a range of styrene contents. The T_g , measured as the mid-point of the change in heat capacity, was $-61 \pm 1^\circ\text{C}$ for all of the samples. The literature values of PIB T_g are approximately -70°C ^{31,32}, while other studies on block copolymers of PIB have shown that a PIB mid-block has a T_g of -65°C ¹⁹. In these results, there is no indication of increasing T_g with decreasing IB contents as would be expected if a broad interface existed. This result is consistent with the observed morphologies where in all cases a sharp interface existed between PS and PIB phases.

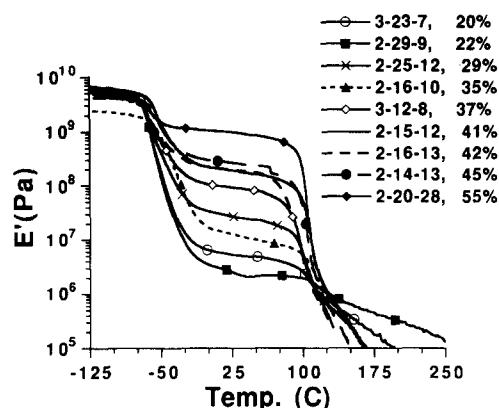


Figure 5 Dynamic modulus (E') as a function of temperature for PS-PIB-PS block copolymers of various compositions

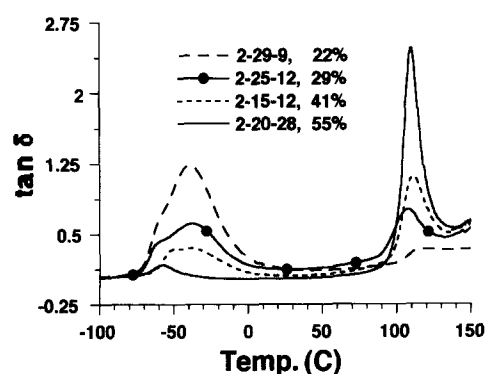


Figure 6 Loss tangent ($\tan \delta$) as a function of temperature for PS-PIB-PS block copolymers of various compositions

Dynamic mechanical properties

The dynamic mechanical properties of PS-PIB-PS block copolymers were studied as a function of polymer composition at a frequency of 1 Hz, from -130°C to a temperature well above the T_g of the PS domains. Figure 5 shows the dynamic modulus (E') and Figure 6 the loss tangent ($\tan \delta$), for some of the samples synthesized. These figures show that all samples possess a dual phase morphology evidenced by two distinct glass transitions corresponding to the PIB and PS phases. This dynamic mechanical behaviour is characteristic of a microphase-separated block copolymer. The figures also demonstrate that the relative intensities of the PIB and PS glass transitions ($\tan \delta$), as well as the rubbery plateau moduli, scale quite well with the copolymer composition. In Figure 5, all of the samples show a glassy region below -65°C . Beginning at -65°C the sample softens and the modulus drops; this corresponds with the T_g measured by d.s.c. The rubbery plateau value of the elastic modulus is reached between 0°C and 20°C , and the plateau extends to approximately 100°C which corresponds to the T_g of the PS block.

Loss tangent vs. temperature curves for representative samples are shown in Figure 6. The complex behaviour of the low temperature (PIB phase) transition is clearly evident. $\tan \delta$ begins to increase at -65°C , which corresponds to the value of the T_g measured by d.s.c. However, the relaxation is quite broad, and for most samples appears to consist of a low temperature component corresponding to the T_g of PIB, and a

Table 4 Dynamic tensile modulus (E') at 25°C as a function of copolymer composition for PS-PIB-PS block copolymer

Sample ID	Vol% PS	E' at 25°C (Pa)
2-29-9	22	2.49×10^6
2-25-12	29	2.69×10^7
2-16-10	35	3.42×10^8
2-15-12	41	1.88×10^8
2-16-13	42	1.95×10^8
2-14-13	45	2.62×10^8
2-20-28	55	9.73×10^8
3-23-7	20	5.26×10^6
3-12-8	37	9.25×10^7

higher temperature component centred at -35°C . The latter is by far the more intense of the two components at high PIB contents. Combined, the entire low temperature mechanical transition has a half width at half maximum on the order of 50°C . This is considerably broader than that found in styrenic block copolymers containing butadiene (15°C)¹ or hydrogenated butadiene (27°C)¹.

The high temperature mechanical transition, corresponding to the T_g of the PS blocks, occurs in the range of 100°C to 125°C . At low styrene contents the relative intensity of the $\tan \delta$ is decreased, but there is no significant sign of broadening in any of the samples. Thus, as with the calorimetric measurements and the microscopy results, no indication of a broad PIB-PS interface is given by the high temperature mechanical relaxation.

The broad nature of the PIB mechanical transition in the block copolymers is an inherent characteristic of PIB. One rheological study of homo-PIB found the chain to have three relaxation processes in the glassy to rubbery transition³³. These results were interpreted according to a cluster model, where each one of the transitions is associated with a cluster type of different rigidity and structural order. A recent inelastic neutron scattering study involved investigation of the chain dynamics of PIB at temperatures above and below the T_g ³⁴. Its results provide evidence for torsional backbone chain motion with a characteristic length ξ . The scattering results indicate that as the temperature increases over T_g , ξ increases, but only slowly with temperature. This would provide a molecular explanation for the appreciable temperature range between the calorimetric T_g and the α -relaxation in PIB. From a molecular point of view, the broad character of the low temperature mechanical relaxation arises from the sterically hindered nature of the PIB backbone, where every other backbone carbon is substituted with two methyl groups.

The values for the elastic modulus at 25°C have been obtained from Figure 5 and are listed in Table 4. In general, the modulus increases with increasing PS content; this is logical since the PS domains serve not only as network junctions but also act as filler particles within the PIB matrix. The modulus of any cross-linked elastomer is expected to be higher in the presence of a rigid filler.

The properties of the block copolymers were found to be more sensitive to processing conditions at higher PS contents. In general, when vol% PS was 35 and higher, elastomeric properties could be significantly improved by annealing solvent-cast films at 110°C for 24 h, in addition

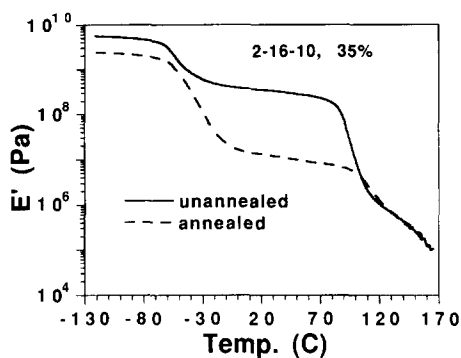


Figure 7 Effect of annealing on the dynamic modulus of PS-PIB-PS block copolymer, 2-16-10

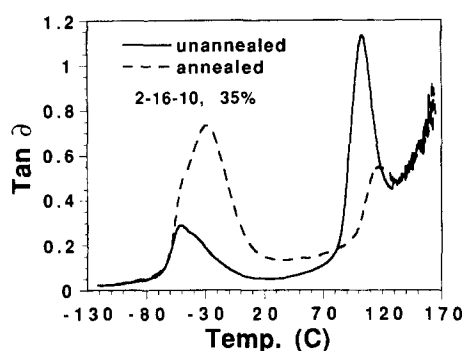


Figure 8 Effect of annealing on the loss tangent of PS-PIB-PS block copolymer, 2-16-10

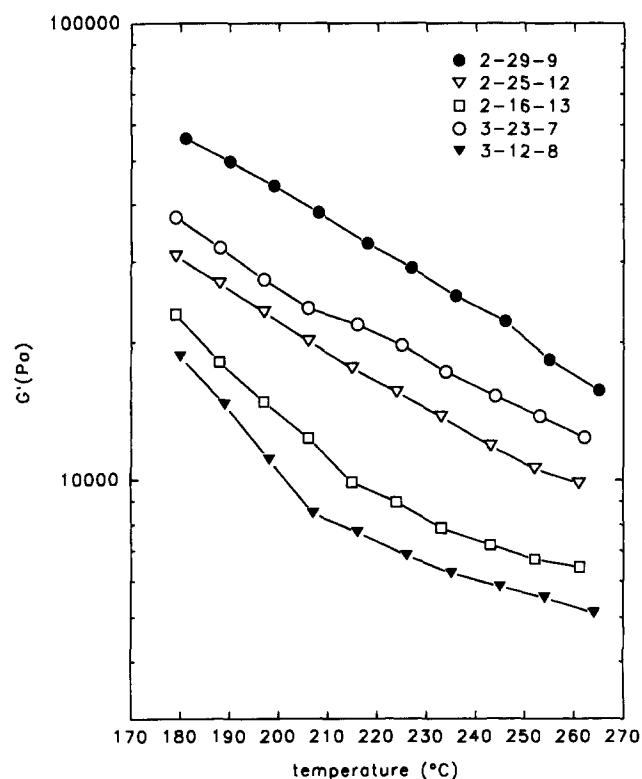


Figure 9 Elastic shear modulus of PS-PIB-PS block copolymers

to the standard curing conditions of 60°C for several days. For example, Figures 7 and 8 compare the dynamic mechanical properties of sample 2-16-10 (35 vol% PS) with and without annealing. The rubbery plateau

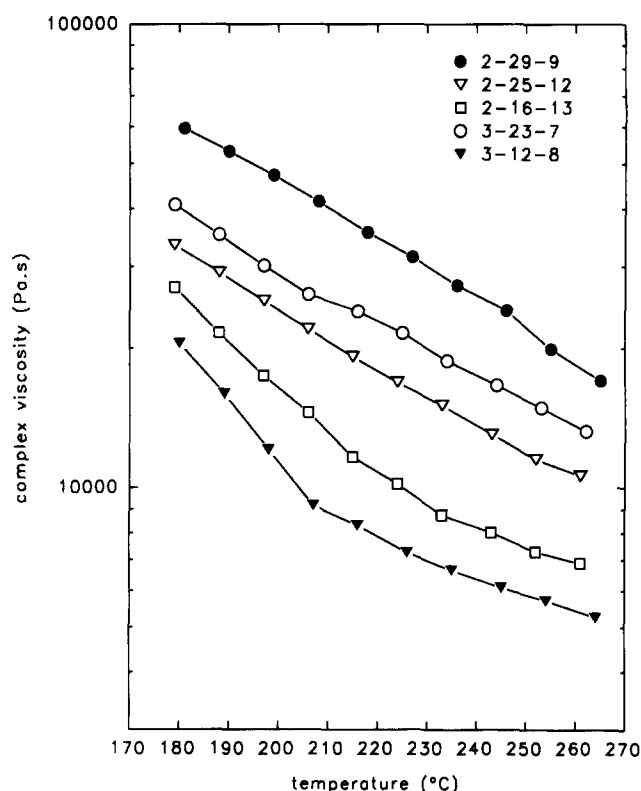


Figure 10 Complex viscosity of PS-PIB-PS block copolymers

modulus dropped significantly upon annealing as shown in Figure 7. As shown in Figure 8, annealing also resulted in a shift to higher temperature and a decrease in intensity of the $\tan \delta$ peak corresponding to the PS domain T_g , and an increase in intensity of the PIB T_g at -60°C . These changes in the dynamic mechanical properties indicate that samples with higher PS contents do not reach equilibrium morphology, even when cast from THF, without being annealed for some period of time above the T_g of PS.

Melt rheology

The melt rheology of these polymers is characteristic of microphase-separated block copolymers. Figures 9 and 10 show the elastic shear modulus and the complex viscosity, respectively, as a function of temperature for five selected samples. All of these polymers show a high value of the elastic modulus up to 265°C . This elasticity is derived from the microphase-separated nature of the melt even at these high temperatures. Melt elasticity is the dominant contribution to the complex viscosity; thus it follows closely the elastic modulus.

The variations among the different samples can be attributed to the molecular weight of the PIB blocks. Both the elastic modulus and the complex viscosity increase with increasing PIB block molecular weight. PS content and morphological type do not seem to have a dominating effect on either G' or η^* .

The phase-separated character of the melts of the five selected polymers was confirmed rheologically up to 265°C . The frequency response was determined between 175 and 265°C , and the data were then superposed by application of a horizontal shift. The result is shown in Figure 11 for sample 2-25-12, whose behaviour was qualitatively representative of these five samples. It is

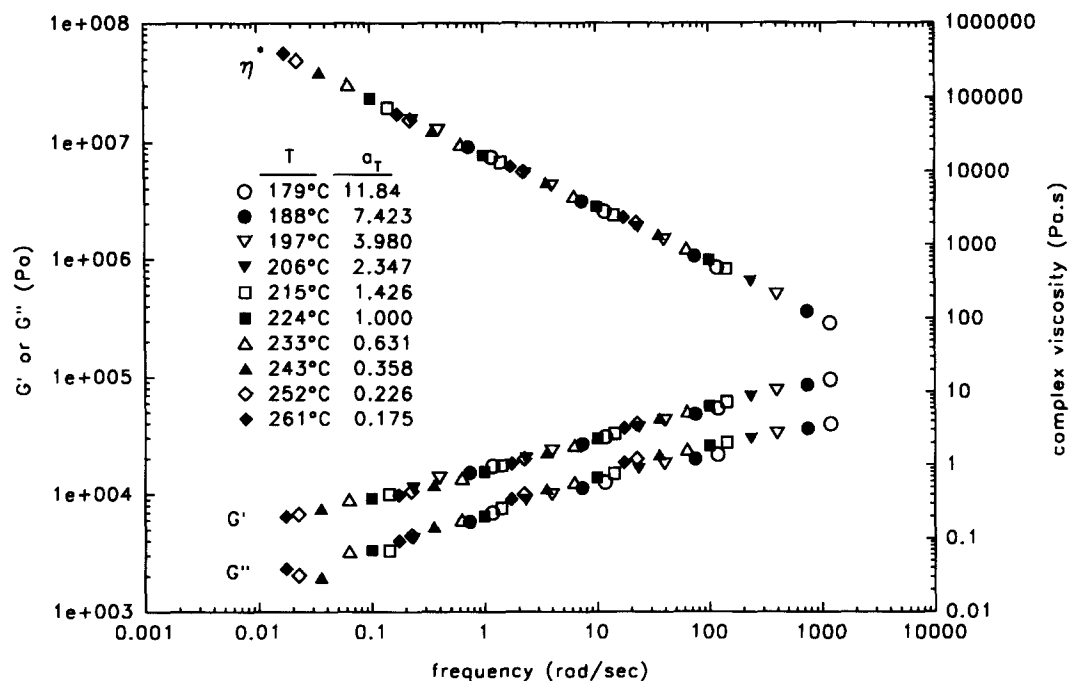


Figure 11 Time-temperature superposed frequency response of 2-25-12

Table 5 Tensile properties of PS-PIB-PS block copolymers

Sample ID	Vol% PS	Stress at break (MPa)	Strain at break (%)	Young's Modulus (MPa)
2-29-9	22	24	906	1
2-25-12	29	13	460	19
2-16-10	35	19	493	60
2-15-12	41	15	372	35
2-16-13	42	8	212	86
2-14-13	45	5.5	85	60
3-23-7	20	19	767	3.5
3-12-8	37	10	339	52

apparent that the viscosity is non-Newtonian over the entire temperature and frequency range tested, and furthermore, both G' and G'' are found to scale as $\omega^{0.28}$ and $\omega^{0.37}$, respectively. This type of rheological test was developed by Bates *et al.*^{35,36} as a tool to determine the phase state of a block copolymer melt. The frequency dependence of G' and G'' are indicative of the phase state of the melt. When the melt is microphase separated, the dynamic moduli both scale to a fractional power of the frequency, most commonly 0.5. As the block copolymer passes through the order-disorder transition, its rheological behaviour becomes that of a homogeneous melt and $G' \sim \omega^{2.0}$ and $G'' \sim \omega^{1.0}$. This is common of homopolymers in terminal zone flow and is predicted by Rouse and generalized Maxwell models of viscoelastic behaviour³⁷. The fractional power frequency dependence of G' and G'' indicates that these samples remained microphase separated up to 265°C. That the order-disorder transition is high in these block copolymers is not unexpected. The strength of phase separation increases, in order, for the series of poly(styrene-butadiene), poly(styrene-isoprene), hydrogenated poly(styrene-butadiene) block copolymers³⁸.

Tensile properties

The tensile properties of the block copolymers were measured on solution cast films at ambient temperature using a strain rate of 1 mm s⁻¹. The values of stress at break, strain at break, and Young's modulus as displayed in Table 5, were determined by taking the average of approximately five 11.0 × 1.54 × 0.50 mm micro-dumb-bell test specimens. Tensile data were not obtained for sample 2-20-28 due to its brittle nature, which caused severe difficulty in cutting micro-dumb-bell test specimens. Sample 2-14-3 was estimated to possess a tensile strength of ~2 MPa, but it was too weak to yield quantitative results on the MTS testing machine.

Figure 12 displays representative stress-strain curves for the samples produced. The results show that these PIB-based block copolymers exhibit strength and toughness comparable to that of diene-based materials synthesized from living anionic polymerization. The properties of PS-PIB-PS block copolymers ranged from very elastomeric, as was the case for samples 2-29-9 and 3-23-7, to that of ductile thermoplastic, as was the case for samples 2-16-13 and 2-15-12. The tensile properties of these materials depend on the block copolymer structure,

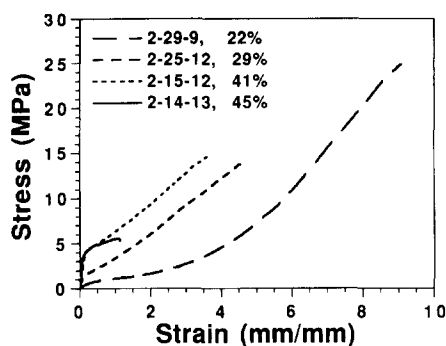


Figure 12 Representative stress-strain curves for PS-PIB-PS block copolymers of various compositions

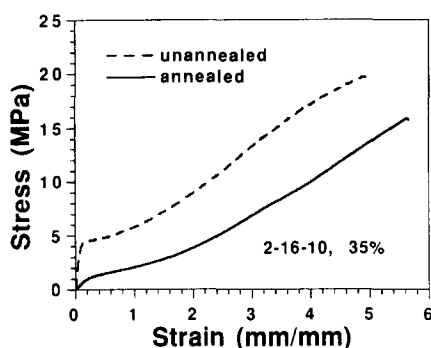


Figure 13 Effect of annealing on the tensile properties of block copolymer 2-16-10

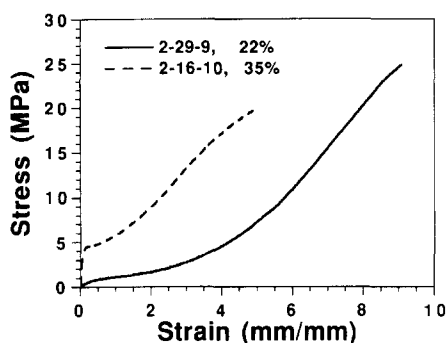


Figure 14 Effect of PIB span molecular weight or vol% PS on the tensile properties of PS-PIB-PS block copolymers

i.e. block lengths, copolymer composition, molecular geometry, and heterophase morphology. For example, small increases in polystyrene content from 15 vol% to 22 vol% caused a dramatic change in the tensile properties, with the tensile strength increasing from ~ 2 MPa to 24 MPa. A similar observation was made by Morton *et al.*³⁹ for poly(styrene-*b*-isoprene-*b*-styrene) block copolymers in which the tensile strength increased from 2.2 MPa for a 19 wt%, 2-30-7 polymer to 16.0 MPa for a 20 wt%, 2-32-8 polymer. In this composition range the morphology changes from spherical to cylindrical PS microdomains; thus, the increase in strength is correlated to the increased dimensionality of the cylindrical PS microdomains.

When the PS content of the copolymers was increased to the range of approximately 35–45 vol%, the tensile properties became characterized by a distinct yield point

followed by a period of cold drawing and then an elastic extension. For higher polystyrene contents, as illustrated by the 45 vol%, 2-14-13 sample, PS-PIB-PS block copolymers exhibited a yield point followed by a short draw and immediate break. The appearance of distinct yield points in these high-PS-content block copolymers can be attributed to the presence of a semi-continuous PS phase, which fractures at the yield elongation⁴⁰. Although microscopy was not performed on the samples of highest PS content, the data in Table 3 show that even at a PS content of 37 vol%, the samples are beginning to exhibit lamellar morphologies in which there exist semi-continuous domains for each block. It is deformation and fracture of semi-continuous PS domains that is responsible for the production of a yield point^{41–43}. As mentioned earlier, it was important that samples of high PS content were annealed, to ensure that an equilibrium morphology had been attained. For example, as shown in Figure 13, when sample 2-16-10 (35 vol% PS) was annealed for 24 h above the T_g of the PS phase, it showed typical elastometric properties with no yield point. However, failure to anneal the sample produced a high initial modulus and yield point, suggesting the presence of a semi-continuous, lamellar PS phase.

As expected, increases in PIB span molecular weight generally led to decreases in modulus and increases in elongation at break. Here, span molecular weight refers to the PIB chain length between two PS blocks. While this quantity is the total PIB molecular weight in linear samples, it is only two-thirds of the total in three-arm star samples. Copolymers 2-29-9 and 2-16-10 provide an excellent illustration of the effect of PIB span molecular weight on tensile properties. These two samples possess similar PS block lengths, but their PIB span molecular weights differ by a factor of 1.8. Naturally, a longer PIB block also causes a decrease in the vol% PS, since the PIB block effectively dilutes the PS domains in the system. As illustrated in Figure 14, increasing the PIB span molecular weight, i.e. decreasing the PS content, decreases the modulus and increases elongation at break.

This effect is examined further in Figure 15, where elongation at break is plotted as a function of the span molecular weight. As the PIB span is increased from approximately 25 000 to 60 000 g mol^{-1} , the elongation at break increases from 150% to 900%. To verify the dominant effect of PIB span molecular weight on elongation at break, a normalized elongation was calculated and plotted against PIB span molecular weight. The normalization procedure consisted of dividing the measured elongation at break by the contour length of the PIB span. Using literature values of the molecular dimensions of PIB⁴⁴, an average repeat unit length of 0.217 nm was calculated. With this and the repeat unit mass of 56 daltons, the contour length was calculated from the PIB span molecular weight for each sample. The results are shown in Figure 16, excluding samples 2-14-13 and 2-16-13, which showed pronounced yielding and failure shortly thereafter. The normalized elongation appears to be a constant with an approximate value of $3.6\% \text{ nm}^{-1}$ with only a small degree of scatter. Importantly, these samples comprised a set with varying PS molecular weight, PS content, and initial morphological type. That the normalized elongation is a constant within this set strongly suggests that the PIB

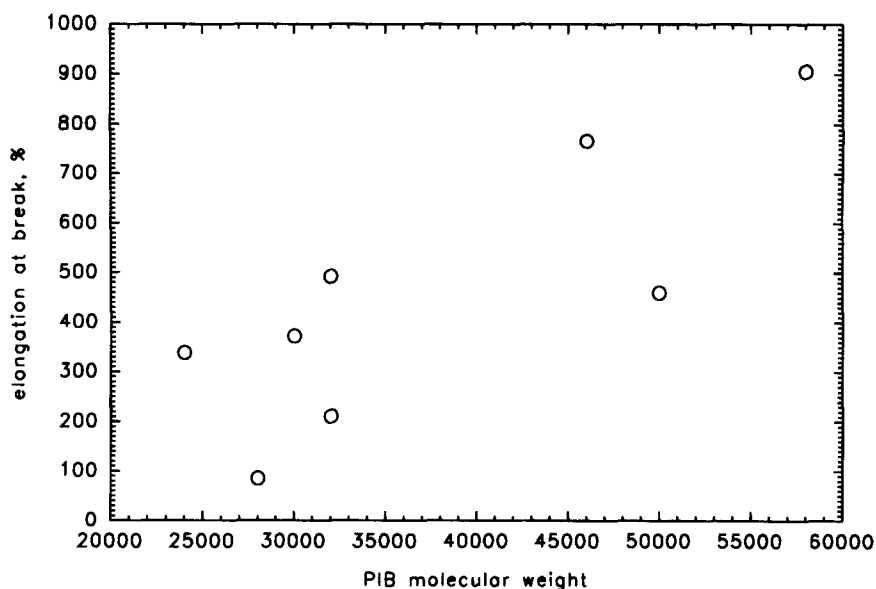


Figure 15 Correlation of elongation at break with PIB span molecular weight

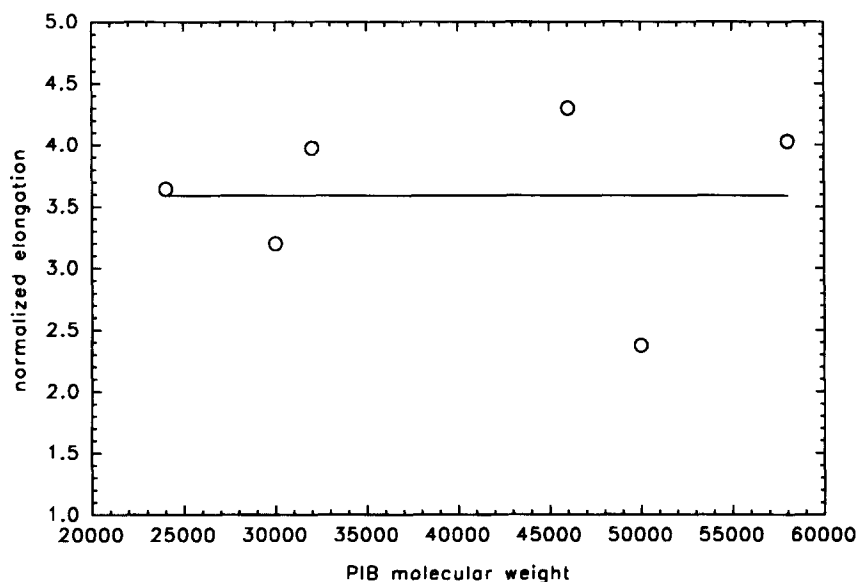


Figure 16 Correlation of normalized elongation at break with PIB span molecular weight

span molecular weight is the dominant variable in determining the elongation at break. On a molecular scale, the chains are elongating until they reach a limiting extension. At this point they mechanically transmit a critical stress across the chain to initiate failure. That the limiting extension is not dependent upon morphological type is reasonable since the long range order and microdomain structure are ruptured at extensions preceding failure^{41,42}. The normalized elongations of the two samples that failed shortly after yielding were significantly lower than $3.6\% \text{ nm}^{-1}$, i.e. 0.8 and $1.7\% \text{ nm}^{-1}$, respectively. This suggests perhaps a different failure mechanism for these samples.

CONCLUSION

The living carbocationic polymerization system employed for this study enabled the synthesis of well defined PS-PIB-PS block copolymers which possessed

morphological and mechanical properties similar to anionically synthesized poly(styrene-*b*-diene-*b*-styrene) block copolymers.

High resolution g.p.c. revealed that the composition of these block copolymers is more complex than initially thought. Coupled species that result from Friedel-Crafts alkylation of styrenyl aromatic rings by living polystyryl chain ends are apparently formed during the later stages of the styrene polymerization step. Both once-coupled ($2\times$ molecular weight) and twice-coupled ($3\times$ molecular weight) species were detected. In addition, at least two lower molecular weight impurities of equivocal origin were revealed, although one is probably homo-PS. The results clearly show that the identity of the low molecular weight impurities are dependent on the particular initiator used, and that most of the impurities result from side reactions during cross-over from living PIB to styrene or during subsequent styrene polymerization.

Within the mid-range of block copolymer composition, i.e. for volume fractions PS in the range 0.20–0.42 vol%, phase morphology, as observed using STEM, was in most cases cylinders of PS in a continuous matrix of PIB. One sample with PS content equal to 29 vol% displayed mixed spherical/cylindrical morphologies, and another with PS at 37 vol% displayed mixed cylindrical/lamellar morphologies. The presence of these mixed morphologies within a compositional regime normally associated with pure cylinders was interpreted to mean the existence of significant compositional inhomogeneities within these particular samples. Additionally, several samples showed evidence of unstained homo-PIB; however, high resolution g.p.c. suggested that most samples were free of homo-PIB. Linear samples showed higher long-range order than three-arm star samples, confirming the expectation that a linear molecule would generally possess greater mobility and ordering tendency during the latter stages of film formation.

Dynamic mechanical analysis revealed that the phase separation in PS-PIB-PS block copolymers is very well defined, when samples were annealed, with no indication of a broad interface. This is quite reasonable considering the inherent immiscibility of PIB and PS, which is greater than for the common poly(styrene-*b*-diene-*b*-styrene) thermoplastic elastomers. Melt rheological measurements indicated that microphase separation persists up to 265°C for a selected group of samples.

Static tensile testing revealed that the block copolymers displayed strengths, up to 24 MPa, when the PIB chain segment was relatively long and the PS content was in the range 20–35 vol%. Below this range, phase separation was apparently inadequate to impart sufficient elasticity. At PS contents above 35 vol%, there was evidence of a semi-continuous, lamellar PS phase that could in some cases be converted into discontinuous cylinders upon annealing.

ACKNOWLEDGEMENTS

Shell Development Co. is acknowledged for the partial support of this research. The research was also supported in part by the National Science Foundation through grant no. EHR-9108767, the State of Mississippi, and The University of Southern Mississippi. The authors additionally wish to thank Kim Choate (USM) for his help in the preparation of some block copolymers, and Greg York and Karen Labat (SDC) for the electron microscopy data.

REFERENCES

- 1 Holden, G. and Legge, N. R. in 'Thermoplastic Elastomers: A Comprehensive Review' (Eds N. R. Legge, G. Holden and H. E. Schroeder), Hanser Publishers, New York, 1987, Chapter 3
- 2 Hashimoto, T., Shibayama, M., Fujimura, M. and Kawai, H. in 'Block Copolymers' (Ed. D. J. Meier), Harwood Academic Publishers, New York, 1983, p. 74
- 3 Miyamoto, M., Sawamoto, M. and Higashimura, T. *Macromolecules* 1984, **17**, 265
- 4 Faust, R. and Kennedy, J. P. *J. Polym. Sci., Polym. Chem. Edn* 1987, **25**, 1847

- 5 Mishra, M. K. and Kennedy, J. P. *J. Macromol. Sci.-Chem.* 1987, **A24(8)**, 933
- 6 Kaszas, G., Puskas, J. E., Kennedy, J. P. and Chen, C. C. *J. Macromol. Sci.-Chem.*, 1989, **A26(8)**, 1099
- 7 Aoshima, S. and Higashimura, T. *Polym. Bull.* 1986, **15**, 417
- 8 Storey, R. F. and Lee, Y. *J. M. S.-Pure Appl. Chem.*, 1992 **A29(11)**, 1017
- 9 Ivan, B. and Kennedy, J. P. *Macromolecules* 1990, **23**, 2880
- 10 Kaszas, G., Puskas, J. E., Chen, C. C. and Kennedy, J. P. *Polym. Bull.* 1988, **20**, 413
- 11 Chen, C. C., Kaszas, G., Puskas, J. E. and Kennedy, J. P. *Polym. Bull.* 1989, **22**, 463
- 12 Gyor, M., Wang, H. C. and Faust, R. *J. M. S.-Pure Appl. Chem.* 1992, **A29(8)**, 639
- 13 Fodor, Zs., Gyor, M., Wang, H. C. and Faust, R. *J. M. S.-Pure Appl. Chem.* 1993, **A30(5)**, 349
- 14 Kaszas, G., Puskas, J. E., Kennedy, J. P. and Hager, W. G. *J. Polym. Sci., Polym. Chem. Edn* 1991, **29**, 427
- 15 Kennedy, J. P. and Kurian, J. *J. Polym. Sci., Polym. Chem. Edn* 1990, **28**, 3725
- 16 Puskas, J. E., Kaszas, G., Kennedy, J. P. and Hager, W. G. *J. Polym. Sci., Polym. Chem. Edn* 1992, **30**, 41
- 17 Tsunogae, Y. and Kennedy, J. P. *Polym. Bull.* 1992, **27**, 631
- 18 Kennedy, J. P., Meguyira, N. and Keszler, B. *Macromolecules* 1991, **24**, 6572
- 19 Kennedy, J. P., Midha, S. and Tsunogae, Y. *Macromolecules* 1993, **26**, 429
- 20 Storey, R. F., Chisholm, B. J. and Lee, Y. *Polymer* 1993, **34(20)**, 4330
- 21 Higashimura, T., Aoshima, S. and Sawamoto, M. *Makromol. Chem., Macromol. Symp.* 1988, **13/14**, 457
- 22 Kaszas, G., Puskas, J. E., Chen, C. C. and Kennedy, J. P. *Macromolecules* 1990, **23**, 3909
- 23 Balogh, L. and Faust, R. *Polym. Bull.* 1992, **28**, 367
- 24 Wang, B., Mishra, M. and Kennedy, J. P. *Polym. Bull.* 1987, **17**, 205
- 25 Kaszas, G., Puskas, J. E. and Kennedy, J. P. *Polym. Bull.* 1987, **18**, 123
- 26 Kaszas, G., Puskas, J. E. and Kennedy, J. P. *Macromol. Symp.* 1988, **13/14**, 473
- 27 Storey, R. F. and Chisholm, B. J. *Macromolecules* 1993, **26**, 6727
- 28 Kaszas, G., Puskas, J. E., Kennedy, J. P. and Hager, W. G. *J. Polym. Sci., Polym. Chem. Edn* 1991, **29**, 421
- 29 Gobran, D. A., Ph.D. Dissertation, University of Massachusetts, 1990
- 30 Thomas, E. L., Kinning, D. J., Alward, D. B. and Henkee, C. S. *Macromolecules* 1987, **20**, 2934
- 31 Flory, P. J. 'Principles of Polymer Chemistry', Cornell University Press, Ithaca, 1953, p. 52
- 32 Lee, W. A. and Rutherford, R. A. 'Polymer Handbook', 2nd Ed., (Eds J. Brandrup, E. H. Immergut), John Wiley & Sons, New York, 1975, p. III-144
- 33 Hill, R. M. and Dissado, L. A. *J. Polymer Sci., Polym. Phys. Edn* 1984, **22**, 1991
- 34 Frick, B. and Richter, D. *Phys. Rev. B* 1993, **47**, 14795
- 35 Bates, F. S. *Macromolecules* 1984, **17**, 2607
- 36 Rosedale, J. H. and Bates, F. S. *Macromolecules* 1990, **23**, 2329
- 37 Ferry, J. D. 'Viscoelastic Properties of Polymers', 3rd Ed., John Wiley & Sons, New York, 1980
- 38 Owens, J. N., Gancarz, I. S., Koberstein, J. T. and Russell, T. P. *Macromolecules* 1989, **22**, 3380
- 39 Morton, M., McGrath, J. E. and Juliano, P. C. *J. Polym. Sci., Part C* 1969, **26**, 99
- 40 Beecher, J. F., Marker, L., Bradford, R. D. and Aggarwal, S. L. *J. Polym. Sci., Part C* 1969, **26**, 117
- 41 Fujimura, M., Hashimoto, T. and Kawai, H. *Rubber Chem. Technol.* 1978, **51**, 215
- 42 Pakula, T., Saijo, K., Kawai, H. and Hashimoto, T. *Macromolecules* 1985, **18**, 1294
- 43 Diamant, J., Williams, M. C. and Soane, D. S. *Polym. Eng. Sci.* 1988, **28**, 207
- 44 Fox, T. G. and Flory, P. J. *J. Am. Chem. Soc.* 1951, **73**, 1909